BOXR1030, an anti-GPC3 CAR with exogenous GOT2 expression, shows enhanced T cell metabolism and improved antitumor activity

Taylor L. Hickman[1*], Eugene Choi[1*], Kathleen R. Whiteman[1,2*], Sujatha Muralidharan[2], Tapasya Pai[1], Tyler Johnson[1], Avani Parikh[1], Taylor Friedman[1], Madaline Gilbert[1], Binzhang Shen[1], Luke Barron[1], Kathleen E. McGinness[1], Seth A. Ettenberg[1], Greg T. Motz[1], Glen J. Weiss[1,2**], Amy Jensen-Smith[2**]

[1]Employees of Unum Therapeutics, Inc. Cambridge, MA USA while work was performed

[2]Current SOTIO, LLC employees

[*]Equal contribution

[**]Corresponding authors

Running head: GOT2 improves CAR antitumor activity

Keywords: Glypican-3, immunometabolism, chimeric antigen receptor, T cell exhaustion, solid tumor

Funding: This work was supported by funding from Unum Therapeutics and SOTIO, LLC.

Corresponding Authors:

Glen J. Weiss, 200 Cambridge Park Dr. Cambridge, MA USA, Phone 617-904-7600, weiss@sotio.com

Amy Jensen-Smith, 200 Cambridge Park Dr. Cambridge, MA USA, Phone 617-904-7600, jensen-smith@sotio.com

Manuscript Details: 4926 words, 6 Figures, 0 tables, 4 Supplementary Figures and 3 Supplementary Tables

Statement of Translational Relevance

Chimeric antigen receptor-based T cell (CAR T) therapeutics have revolutionized the field of oncology. Despite early successes targeting hematological malignancies, substantial challenges limit application of CAR T therapy in solid tumors, in part due to the suppressive tumor microenvironment which drives T cell exhaustion and metabolic dysfunction. Glutamic-oxaloacetic transaminase 2 (GOT2) is a mitochondrial enzyme in glutamine metabolism and contributes to cellular redox balance.

Glypican-3 (GPC3) is an oncofetal tumor antigen with restricted expression on normal tissues and high prevalence in several solid tumors. We describe BOXR1030, a novel CAR T therapeutic co-expressing GPC3-targeted CAR and exogenous GOT2. Compared to T cells expressing CAR alone, BOXR1030 T cells demonstrated superior *in vivo* efficacy and have favorable attributes including enhanced cytokine production, a less-differentiated phenotype with lower expression of exhaustion markers, and an enhanced metabolic profile. These data support BOXR1030 as a potential treatment to explore in select solid tumor indications.

Abstract

Purpose: The solid tumor microenvironment (TME) drives T cell dysfunction and inhibits the effectiveness of immunotherapies such as chimeric antigen receptor-based T cell (CAR T) cells. Early data has shown that modulation of T cell metabolism can improve intratumoral T cell function in preclinical models.

Experimental Design: We evaluated GPC3 expression in human normal and tumor tissue specimens. We developed and evaluated BOXR1030, a novel CAR T therapeutic co-expressing glypican-3 (GPC3)-targeted CAR and exogenous glutamic-oxaloacetic transaminase 2 (GOT2) in terms of CAR T cell function both *in vitro* and *in vivo*.

Results: Expression of tumor antigen GPC3 was observed by immunohistochemical staining in tumor biopsies from hepatocellular carcinoma, liposarcoma, squamous lung cancer, and Merkel cell carcinoma patients. Compared to control GPC3 CAR alone, BOXR1030 (GPC3-targeted CAR T cell that co-expressed GOT2) demonstrated superior *in vivo* efficacy in aggressive solid tumor xenograft models, and showed favorable attributes *in vitro* including an enhanced cytokine production profile, a less-differentiated T cell phenotype with lower expression of stress and exhaustion markers, an enhanced metabolic profile and increased proliferation in TME-like conditions.

Conclusions: Together, these results demonstrated that co-expression of GOT2 can substantially improve the overall antitumor activity of CAR T cells by inducing broad changes in cellular function and phenotype. These data show that BOXR1030 is an attractive approach to targeting select solid tumors. To this end, BOXR1030 will be explored in the clinic to assess safety, dose-finding, and preliminary efficacy (NCT05120271).

Introduction

Chimeric antigen receptor-based T cell (CAR T) therapeutics have revolutionized the field of oncology, and have provided substantial benefits to heavily pretreated and treatment refractory patients(1). Despite early successes targeting hematological malignancies, substantial efficacy and safety challenges limit broad application of CAR T therapy in solid tumors(2–4). In the solid tumor microenvironment, CAR T efficacy is limited by cellular suppressive factors such as myeloid-derived suppressor cells, T-regulatory cells and inhibitory receptors (e.g. programmed-death-ligand 1 [PD-L1]) and non-cellular suppressive factors. Nutrient competition within the tumor microenvironment (TME) has been shown to limit the efficacy of checkpoint inhibitor therapies and cellular therapeutics such as CAR T therapy(5,6).

Nutrient competition between tumor cells and T cells has been demonstrated to be a driving force for the development of T cell exhaustion in mouse models of cancer(7). Changes in T cell metabolism have been identified as an initial step in the development of T cell exhaustion in the TME(8). Dysfunctional T cells isolated from human tumors have been described to have broad metabolic defects in both glycolysis and mitochondrial activity(9). T cell metabolism is increasingly recognized as a key contributor to multiple aspects of T cell biology, influencing effector functions(10), differentiation state and memory formation(11,12), and survival(13). Thus, modulation of T cell metabolism could improve T cell function and potentially improve human CAR T cell therapy for cancer.

Glutamic-oxaloacetic transaminase 2 (GOT2, formerly mitochondrial aspartate aminotransferase, mAspAT) is a mitochondrial enzyme that has an essential role in glutamine metabolism as part of the malate-aspartate shuttle. GOT2 catalyzes the production of alpha-ketoglutarate (aKG) and aspartate from glutamate and oxaloacetic acid, feeding the TCA

(tricarboxylic acid, Krebs) cycle and contributes to the maintenance of cellular redox balance(14,15). Although little is known about the role of GOT2 in T cells, growing evidence suggests that GOT2 may be a key factor for optimal T cell activity. T cells from GOT2 knockout mice have impaired IFNγ production(16). In addition, both aKG and aspartate, metabolic products of the GOT2 enzymatic reaction, are involved in essential T cell processes including proliferation and differentiation(16,17). GOT2 is expressed in activated T cells(18), and protein expression is decreased in chronically stimulated T cells(19), which leads us to hypothesize that sustained over-expression of GOT2 may improve CAR T cell function within the solid TME.

Glypican-3 (GPC3) is an oncofetal tumor antigen that is an attractive target for CAR T cell therapy due to its highly restricted expression on normal tissue and high prevalence in several adult and pediatric solid tumors(20). Glypicans are membrane-bound heparin sulfate proteoglycans, known to stimulate or inhibit growth factor activity and are expressed during development in a cell- and tissue-specific manner. GPC3 is involved in regulation of cell proliferation and apoptosis in normal development during embryogenesis and expression is largely absent in normal adult tissues. Aberrant GPC3 expression is implicated in tumorigenesis(21–23), and GPC3-positive cancers including hepatocellular carcinomas (HCC), are characterized by a highly metabolic and immunosuppressive landscape(24), and exhaustion is a common feature of tumor-resident T cells(25).

Here, we describe BOXR1030, a novel CAR T therapeutic co-expressing a GPC3-targeted CAR and exogenous GOT2. GPC3 protein expression was observed in >30% of samples from patients with HCC, squamous cell carcinoma of the lung (SCC), Merkel cell carcinoma (MCC), and liposarcoma demonstrating its attractiveness as a CAR tumor antigen target. Compared to T cells expressing CAR alone, BOXR1030 T cells demonstrated superior *in*

vivo efficacy and have favorable attributes including an enhanced cytokine production profile, a less-differentiated phenotype with lower expression of exhaustion markers, and an enhanced metabolic profile. The data herein support the generation of a GPC3 targeted CAR for the treatment of select solid tumor indications and demonstrate that modulation of T cell metabolism is a promising new approach to improve CAR T cell therapy for the treatment of solid tumors.

Materials and Methods

Ethics

Peripheral blood mononuclear cells (PBMCs) from healthy male and female human donors were obtained from HemaCare. PBMCs were isolated from leukopaks collected in HemaCare's FDA-registered collection centers following cGMP and cGTP collection guidelines from IRB-consented donors. All animal studies accounted for the minimal number of animals required for scientific rigor, and all studies were conducted in accordance with experimental protocols reviewed and approved by the Institutional Animal Care and Use Committee (IACUC) at Unum Therapeutics and/or SOTIO, LLC.

Chimeric Antigen Receptor Constructs and Virus Production

The GPC3 CAR construct (CAR) utilized is composed of a humanized anti-GPC3 targeted single chain variable fragment, CD8-alpha transmembrane domain, and intracellular 4-1BB costimulatory and CD3-zeta signaling domains. The BOXR1030 expression constructs encode both the GPC3 CAR and GOT2, separated by a ribosomal porcine teschovirus 2A (P2A) self-cleaving peptide sequence. Constructs were cloned into the γ-retroviral vector MP71(26). CAR and BOXR1030 encoding MP71 retroviral vector plasmids were transiently transfected into HEK293RTV cells along with packaging plasmids encoding Gag, Pol, and GaLV viral proteins. GaLV-pseudotyped retroviral supernatant was harvested, filtered, and frozen approximately 24 and 36 hours after transfection.

T Cell Transduction and Expansion

CAR transduced T cells were generated using two methods. The first process generated research scale material, while the second process generated good manufacturing practice (GMP)

analogous material. GMP analogous material was used in the safety/biodistribution study, while research scale material was used in all other evaluations (Supplementary Data).

Cell Lines and Additional Assays

Cell line details along with methods for immunohistochemistry (IHC), real-time PCR analysis, Western blot analysis, flow cytometry, aspartate assay, RNA sequencing, and xenograft *in vivo* studies are in the Supplementary Data.

GPC3 expression from public databases

RNA-sequencing profile of GPC3 expression in patient tumors from selected indications were generated in whole by the TCGA (The Cancer Genome Atlas) Research Network. Data were accessed using the cBioPortal for Cancer Genomics hosted by the Center for Molecular Oncology at Memorial Sloan Kettering(27,28). Data for selected indications was downloaded from cBioPortal on January 8, 2021 and visualized using GraphPad Prism 9 software. mRNA expression is reported as RSEM (batch normalized from Illumina HiSeq_RNASeqV2) (log2(value + 1)). The RNA expression profile for GPC3 (ENSG00000147257.13) in normal human tissues was accessed from the Genome-Tissue Expression Project (GTEx) analysis release V8 (dbGaP Accession phs000424.v8.p2) on September 24, 2021 via the GTEx portal (https://gtexportal.org/home/). Data are reported as transcripts per million (TPM) and box plots are shown as the median and 25th and 75th percentiles. Points are displayed as outliers if values are greater than or less than 1.5 times the interquartile range.

Statistical analyses

Data Analysis and statistical comparisons were made using Prism 8 (GraphPad Software, San Diego, CA.). Statistical comparisons were determined by the nature of data and are specifically described within figure legends. In general, comparison between two groups were determined by

Student's *t* tests, often paired for each donor. Multiple comparisons were performed by a one-way analysis of variance (ANOVA), followed by Tukey's multiple comparison test post-hoc. Correlations were determined by Pearson's test. Statistical methods for RNA-Seq analysis are described in the Supplementary Data. Statistical significance was defined as $p<0.05$.

Results

Expression profile of GPC3 in human normal and tumor tissue specimens

GPC3 expression has been reported at very low levels in limited normal tissues (20). To confirm these results, GPC3 mRNA and protein expression was assessed in primary human non-disease tissues. GPC3 mRNA expression profile was queried from the GTEx RNAseq database representing 54 tissue sites from ~1,000 patient samples via the GTEx portal. GPC3 mRNA was expressed at low levels predominantly in lung, adipose, tibial nerve, kidney and breast (Supplementary Figure 1A). GPC3 protein expression by IHC in a tissue microarray (TMA) (adipose and tibial nerve not represented) showed predominantly faint, cytoplasmic staining in a few tissues including heart, kidney and stomach and no expression in lung or breast (Figure 1A, Supplementary Data).

GPC3 mRNA and protein expression was also assessed in primary human tumor samples for selected indications. RNAseq data profiling GPC3 expression in HCC, SCC, liposarcoma, colorectal adenocarcinoma (CRC), and serous ovarian cancers (OC) was accessed from the Cancer Genome Atlas Program (TCGA) and showed varying degrees of GPC mRNA expression (Supplementary Figure 1B). To determine the prevalence of GPC3 positive tumors, we performed GPC3 IHC staining of TMAs in the same indications (Supplementary Table 1A). No appreciable expression was observed in CRC or OC with <10% cases exhibiting an H-score ≥ 30. However, HCC, SCC, and myxoid/round liposarcoma (MRCLS) samples in the TMAs showed appreciable levels of GPC3 expression (H-score ≥ 30) with >20% prevalence (Supplementary Table 1A). Additionally, we performed IHC on 20-40 unique tumor samples for each of these four indications: HCC, SCC, liposarcoma, as well as, MCC(21). These additional results showed positive GPC3 staining (H-score ≥ 30) in >30% cases (Figure 1B, Supplementary

Table 1B). Overall, HCC, SCC, MRCLS, and MCC had a prevalence of 69%, 33%, 33%, and 70% respectively. These data support the generation of an GPC3 targeted CAR for the treatment of these solid tumor indications.

BOXR1030 T cells co-express exogenous GOT2 and a GPC3-targeted CAR

We designed a 2nd generation CAR containing a humanized GPC3-targeting scFv, 4-1BB costimulatory domain, and a CD3ζ signaling domain. Codon optimized GOT2 was co-expressed in the same construct using a P2A sequence to evaluate the impact of modulation of T cell metabolism on CAR T cell function, referred to as BOXR1030 herein (Figure 2A).

BOXR1030 T cells or control T cells expressing the GPC3-targeting CAR alone, were generated by activating normal human donor PBMCs with anti-CD3 and anti-CD28 and transducing with gamma retrovirus. T cells were assessed after 10 days for CAR and GOT2 transgene expression. GPC3 CAR was expressed at similar levels in both control CAR and BOXR1030 CD3+ T cells (Figure 2B and C). CAR expression was also equivalent in CD4+ and CD8+ T cell populations in both control and BOXR1030 T cells (Figure 2C). To distinguish between endogenous and exogenous GOT2, qRT-PCR primers were designed to specifically detect the wild-type and codon optimized GOT2 sequences. Endogenous GOT2 mRNA expression was detected at similar levels in both control CAR T cells and BOXR1030 cells, whereas exogenous GOT2 mRNA levels were only detected in BOXR1030 T cells and at levels significantly higher than endogenous GOT2 mRNA (Figure 2D).

GOT2 protein levels were measured by Western blot. Because endogenous and exogenous protein have the same amino acid sequence, they are indistinguishable. Despite detecting high levels of mRNA expression in BOXR1030 T cells, there was no apparent

difference in protein expression at baseline compared to control CAR T cells (Supplementary Figure 2A). However, when T cells were stimulated with plate bound GPC3 antigen for six days, an increase in GOT2 protein expression was observed in a time dependent manner in BOXR1030 T cells, while GOT2 expression in control CAR T cells remained unchanged (Supplementary Figure 2A). Similarly, exogenous GOT2 mRNA expression increased in BOXR1030 T cells following stimulation and directly correlated with an increase in GPC3 CAR scFv mRNA expression (Supplementary Figure 2B-D). Taken together, these data demonstrate GPC3 CAR and GOT2 expression in BOXR1030 T cells that is maintained throughout 7 days post T cell activation.

We next evaluated T cell phenotype in CD8+CAR+ and CD4+CAR+ T cells from BOXR1030 and control CAR T cells. CD45RA and CD27 are surface markers associated with T cell memory and differentiation state. BOXR1030 T cells had a greater frequency of CD8+CAR+ T cells with a less-differentiated naïve phenotype (CD45RA+CD27+) relative to control CAR T cells and corresponding decreases in more differentiated central memory (CD45RA-CD27+), effector memory (CD45RA-CD27-), and effector memory-like (CD45RA+CD27-) populations (Figure 2E). A similar, but less pronounced trend was observed in CD4+CAR+ T cells with a significant increase in the less-differentiated CD45RA+CD27+ population (Figure 2E). Taken together these results suggest that BOXR1030 T cells may have a less differentiated and therefore more favorable phenotype compared to T cells expressing CAR alone.

Exogenous GOT2 overexpression enhances intracellular aspartate and aspartate aminotransferase (AST) activity

GOT2 catalyzes the production of aspartate and aKG (14,15) (Figure 3A). To confirm function of exogenously expressed GOT2, we measured aspartate and aKG levels in control CAR and BOXR1030 T cells. aKG levels were below the limits of detection of the assay (data not shown), however we were able to detect a significant increase in intracellular aspartate in BOXR1030 T cells relative to control CAR T cells (Figure 3B). AST enzymes include GOT1 and GOT2 and catalyze the reversible conversion of oxaloacetate (OAA) and glutamate into aspartate and αKG, respectively. To further confirm activity of GOT2, BOXR1030 and CAR control T cells were activated with GPC3+ Hep3B target cells for 8 days to evaluate the contribution of GOT2 to AST activity. Although magnitude of activity varied between experiments, overall greater AST activity was observed in BOXR1030 T cells relative to controls (Figure 3C). In summation, exogenous expression of GOT2 in BOXR1030 T cells results in increased AST activity and intracellular aspartate consistent with an enhanced metabolic phenotype compared to T cells expressing CAR alone.

BOXR1030 has enhanced in vitro activity under TME-like stress conditions

In vitro activity of BOXR1030 and CAR control T cells was evaluated in co-culture with tumor cell lines. Cytokine secretion, cytotoxicity, and T cell proliferation were measured in response to a panel of cell lines expressing high, medium, and low levels of the GPC3 target antigen to determine whether *in vitro* activity was dependent on antigen expression level (Figure 4A and B). BOXR1030 T cells performed similarly to control CAR T cells in all assays, indicating comparable CAR function in the presence of GOT2 transgene under standard *in vitro* assay conditions (Figure 4C-H). IFN-gamma release was observed against all target expressing cell lines regardless of high, medium, and low GPC3 expression levels (Figure 4C). IL-2, TNF-

alpha, and IL-17A release was observed with high and medium GPC3 expressing lines, and decreased levels were observed with the low GPC3 expressing target cell lines (OV90 and SNU398) (Figure 4D-F). PLC/PRF/5 cell line has overall low GPC3 expression, however expression is heterogenous in this cell line with populations ranging from negative to high expression (Figure 4B), which may explain higher levels of activity of response with this cell line.

Based on the slightly different cell phenotypes observed in CD4+ and CD8+ BOXR1030 cells (Figure 2E), we also evaluated the ability of CD4+ and CD8+ CAR+ T cells to produce TNF-α, IFN-γ, IL-2, and IL-17A following stimulation with GPC3+ target cells by intracellular cytokine staining. Relative to control CAR CD4+ T cells, we observed a significant increase in the proportion of BOXR1030 CD4+ T cells that produced IL-17A, IFN-γ, or TNF-α (Fig 4I). These changes were more pronounced within the CD4+ subset, and within the CD8+ subset, we observed no difference for either IFN-γ or IL-17A and a slight decrease in TNF-α+ and IL-2+ CD8+ BOXR1030 T cells (Fig 4I). This suggests increased numbers of pro-inflammatory Th1 and Th17 CD4+ T cells which can, in addition to augmenting anti-tumor cytotoxic responses by CD8+ T cells, mediate direct anti-tumor activity by the production of cytokines (34,35).

T cell cytolytic activity was comparable across all target antigen densities (Figure 4G), whereas T cell proliferation was greater in high and medium GPC3 expressing lines compared to low expressing lines (Figure 4H). A threshold of GPC3 expression for activation of BOXR1030 T cells was not identified, however diminishing levels of activity were observed in low GPC3 antigen cell lines. Importantly, no reactivity was observed against a panel of GPC3 negative cell lines confirming specificity of the GPC3 CAR for its target antigen (Supplementary Figure 3A-E).

To further test BOXR1030 T cells *in vitro*, CAR T cells were assessed under conditions of chronic antigen stimulation in the presence of limited oxygen or nutrients to mimic the solid TME. BOXR1030 or control CAR T cells were co-cultured with either Hep3B or JHH7 target cells under TME-stress conditions and proliferation was measured by geometric mean fluorescence intensity of the intravital fluorescent dye, CellTrace Violet (CTV), where signal decreases with increased cell division. BOXR1030 T cells had consistently improved proliferation when restimulated with either Hep3G or JHH7 target cells under hypoxic conditions compared to control CAR T cells (Figure 5A). Similarly, BOXR1030 T cells also outperformed control CAR T cells in response to chronic stimulation in low glucose conditions (Figure 5B). Taken together, these data suggest that BOXR1030 T cells may have a proliferative advantage within the solid TME.

Exogenous GOT2 overexpression alters the transcriptional profile of CAR T cells

We next evaluated the transcriptional profile of BOXR1030 T cells compared to CAR T cells at baseline and 4 and 24 hours after stimulation with immobilized recombinant GPC3 protein. T cell activation makers *CD69*, *CD154 (CD40LG)*, *IL2RA (CD25)*, and *PDCD1 (PD1)* mRNA were all elevated at 4 hours compared to baseline and returned to levels at or below baseline within 24 hours except for *CD69* which remained elevated 24 hours post stimulation. There were no differences in expression of the selected activation markers between control CAR T cells and BOXR1030 T cells (Supplementary Figure 4A).

Transcriptional differences were observed across time points following stimulation (Supplementary Table 3). Relative to the control CAR T cells, we observed significantly lower levels of genes involved in the response to cellular stress, notably *HSP90AA1*, *HSPE1*, *HSPA1A*, *HSPB1* and the related genes *AHSA1* and *FKBP4* (Supplementary Figure 4B-E; and

Supplementary Table 3) at baseline and following activation. We also observed lower levels of the transcription factor *TOX2* in BOXR1030 T cells relative to CAR T cells. *TOX2* is a member of the TOX family of transcription factors which have recently been implicated in the development of T cell exhaustion, and knockout of TOX2 in T cells improved their antitumor activity and survival(29,30). Interestingly, we also observed down regulation of *SOX4*, which has been shown to be down regulated in TOX knockout T cells(29). These data suggest that BOXR1030 cells exhibit a transcription profile consistent with reduced cellular stress and exhaustion compared to control CAR T cells.

We also observed increases in RNA levels of CD4+ T cell subset Th17 related genes such as *IL-17A/F*, as well as, CD8+ effector memory related genes such as chemokine receptor *CX3CR1*(31) in BOXR1030 cells. We extended our studies to evaluate BOXR1030 CD4+ and CD8+ T cell subsets separately. RNA levels of genes in the heat shock protein family and exhaustion related genes *TOX2* and *SOX4* were lower in both BOXR030 CD4+ and CD8+ T cell subsets (Supplementary Figure 4F and G; and Supplementary Table 2); however, select changes were restricted to a given T cell subset. For example, increases in *IL-17A/F* were restricted to the CD4+ subset, along with increased *RORC* which is a Th17 master transcription factor, implicating a possible enrichment of Th17 CD4+ T cell subsets in BOXR1030 T cells which is consistent with the previous intracellular cytokine staining data (Figure 4I). The significance of Th17 cells in anti-tumor responses has been complicated by conflicting reports. However, in the context of adoptive cell therapy such as CAR T cells, Th17 cells have exhibited persistence *in vivo*, displayed resistance to activation-induced cell death, and possessed robust recall responses which could support a more potent anti-tumor response(32).

We next examined changes in pathways between CAR and BOXR1030 at baseline and after 4 hours of activation, using single sample gene set enrichment analysis (ssGSEA). Consistent with our differential gene expression analysis, we observed downregulation of pathways associated with responses to metabolic, environmental, and oxidative stress. Notably, we observed a reduction in the pathway enrichment for genes associated with protein refolding and mTOR signaling (Supplementary Figure 4H and I). mTOR serves as a central regulator of cell metabolism, survival and response to stress, and plays essential roles in T cell memory formation(33). Previous reports have shown that reduction in mTORC1 activity leads to decreased glycolysis and prevents T-cell differentiation which can result in less-differentiated stem cell memory T cell phenotypes(34). Taken together, gene expression changes imply that BOXR1030 T cells may have reduced levels of cellular stress and T cell exhaustion compared to CAR alone control T cells.

GOT2-expressing CAR T cells have substantially improved in vivo antitumor activity associated with reduced inhibitory receptor expression

We next evaluated the *in vivo* efficacy of CAR T cells. In order to meaningfully compare control CAR and BOXR1030 T cells, we developed two stringent xenograft tumor model systems. Our first model system, Hep3B HCC xenograft model, evaluates the intrinsic ability of small numbers of CAR T cells to expand, function, and persist through chronic stimulation and has been termed an "*in vivo* stress test"(35). When low doses of 1 x 10^6 CAR-positive T cells were administered twice, the CAR has little to no antitumor activity (Figure 6A). In contrast, 1 x 10^6 BOXR1030 given twice, led to sustained, durable regressions (~100 days) for all mice treated and was well-tolerated (Figure 6A). This improved antitumor activity was associated with

greater T cell expansion and long-term persistence of BOXR1030 T cells in the blood (Figure 6C), an observation consistent with a less differentiated T cell phenotype and reduced T cell exhaustion. We also evaluated a JHH7 xenograft model with intrinsic resistance to CAR function. With 5 x 10^6 CAR+ cells administered weekly for 2 weeks, BOXR1030 demonstrated dose-dependent peripheral blood expansion and persistence (not shown) which correlated with antitumor activity against GPC3+ xenografts (Figure 6B).

To better characterize the T cell response leading to improved activity of BOXR1030 T cells, we selected the JHH7 xenograft model based on pilot adoptive transfer studies where we observed a relatively large influx of T cells into the tumor in the CAR group, allowing sufficient recovery for flow cytometry analysis. Prolonged exposure to the solid tumor microenvironment leads to metabolic and functional T cell exhaustion, an inhibitory program that limits the efficacy of T cells in the TME(36). This functional exhaustion is often phenotypically marked by the upregulation and subsequent co-expression of multiple inhibitory receptors. To that end, we characterized PD-1 and TIM-3 (T cell immunoglobulin and mucin domain-containing protein 3) inhibitory receptor expression on tumor infiltrating T cells at an early (day 6 or 7) time point where upregulation of PD-1 and TIM-3 are expected with T cell activation, and at a late (day 13 or 14) time point where co-expression of these receptors negatively regulate T cell activation and correlate with T cell exhaustion. BOXR1030 T cells demonstrated a higher frequency of CD4+ and CD8+ T cells co-expressing PD-1 and TIM-3 at the early time point, consistent with an activation phenotype (Figure 6D). At the later time point, CD8+ T cells of the BOXR1030 group, and not CD4+ T cells, demonstrated a significant decrease in co-expression of PD-1 and TIM-3 (Figure 6D). Importantly, expression of PD-1 and TIM-3 on CD8+ T cells, as well as on CD4+ T cells, were positively correlated to tumor volume on day 14 and supports the concept

that sustained inhibitory receptor expression is associated with lack of antitumor activity. Taken together, limited expression of inhibitory receptors and sustained antitumor efficacy suggest that exogenous GOT2 overexpression may allow GPC3-targeted CAR T cells to resist T cell exhaustion when exposed to the solid tumor microenvironment.

In vivo safety, pharmacokinetics and biodistribution of BOXR1030

A non-GLP (Good Laboratory Practice) safety and biodistribution study of GMP-analogous BOXR1030 was conducted at Charles River Research Laboratories (Durham, N.C.). Mice bearing established subcutaneous JHH7 GPC3+ xenografts were treated with a dose of 5 x 10^6 BOXR1030+ T cells on days 1 and 8. There was no indication of toxicity; hematology and clinical chemistry values were in normal range, and no tissue toxicity was detected by histopathologic analysis (data not shown). Peripheral blood pharmacokinetics analyzed by flow cytometry show a peak of circulating BOXR1030+ T cells at day 15 (~50 cells/uL blood) with about a 5-fold decrease in circulating BOXR1030+ T cells (~10 cells/uL) by day 45 (data not shown). Next, we evaluated tissue distribution of BOXR1030+ T cells was analyzed by qPCR, expressed as copies per 100 ng extracted DNA. Minimal BOXR1030+ T cells were detected in brain, heart, kidney and ovaries with reduced counts at the later time point, with an average of 708 copies/100 ng DNA at day 15 and 368 copies/100 ng DNA on day 45. The more highly vascularized tissue group (liver, lung and spleen) had a greater distribution of BOXR1030+ T cells, which also demonstrated clearance over the time points with an average of 11,716 copies/100 ng DNA at day 15 and 6,840 copies/100 ng DNA on day 45. BOXR1030+ T cells were target specific, with approximately 10-fold higher accumulation in tumor tissue compared to the liver, spleen, and lung on day 15 (average 112,963 copies/100 ng tumor DNA). Only one

animal had tumor tissue on day 45, and copy number in the tumor tissue at that time was comparable to liver, lung and spleen. Figure 6E shows BOXR1030+ T cells tissue and tumor distribution at day 15 and 45 post treatment.

The diminishing counts of BOXR1030 in tissue and blood over the time course of the study demonstrate that BOXR1030 does not continue to expand in the absence of GPC3+ target, supporting the target specificity and absence of antigen-uncoupled proliferation of BOXR1030. Thus, there was no indication of toxicity due to BOXR1030, and there was no indication of off-target expansion in normal mouse tissues. BOXR1030 expansion in GPC3+ tumor tissues was observed, demonstrating the target-specificity of BOXR1030.

Discussion

In this study, we characterize BOXR1030 cells expressing GPC3-targeted CAR and GOT2 for the treatment of solid tumor indications and demonstrate that modulation of T cell metabolism can improve CAR T function in an immunosuppressive TME. GPC3 target expression analysis shows protein was expressed in >30% of cases in HCC, SCC, MRCLS and MCC solid tumor indications, and where applicable is consistent with mRNA expression in these indications. Normal tissue mRNA expression is consistently low across nearly all tissues assessed, with highest levels noted in lung, adipose, and tibial nerve; however, GPC3 protein expression by IHC confirms low and predominantly cytoplasmic localization in normal tissues making GPC3 an attractive CAR tumor antigen target.

Solid tumors are characterized by a highly metabolic and immunosuppressive microenvironment(24), and T cell exhaustion is a common feature of tumor-infiltrating T cells(25). Loss of oxidative metabolism due to reduced mitochondrial biogenesis in T cells within the TME has been observed (36). In addition, direct ligation of PD-1 on T cells can lead to broad metabolic reprogramming associated with impairment in glycolysis and amino acid metabolism(37). Activated T cells require large amounts of glucose(38) and amino acids to support biosynthesis and proliferation (10,13,16,39). Competition for nutrients within the TME has been described as a primary factor resulting in loss of T cell function(7). Thus, metabolic impairment is emerging as a key mechanism of T cell immunosuppression exhaustion within the TME.

GOT2 is a well-described mitochondrial enzyme that supports several aspects of cellular metabolism. It is expressed in activated T cells(18), and is downregulated in chronically stimulated T cells(19). In this study, we tested the effect of overexpression of exogenous GOT2

in combination with GPC3 CAR (BOXR1030 T cells) on *in vitro* and *in vivo* CAR T cell phenotype and function compared to GPC3 CAR control T cells. BOXR1030 T cells had increased levels of aspartate and AST activity confirming GOT2 functionality in these cells. In comparing BOXR1030 cells to CAR alone control cells, overall cytokine production, proliferation, and cytotoxicity under standard conditions were similar *in vitro*. However transcriptomic and intracellular protein analysis showed increased levels of Th1/Th17 related cytokines (IFNγ+, IL-17+) in CD4+ T cells expressing BOXR1030 compared to control CAR cells suggesting enhanced cytokine production profile *in vitro*. The differences in cytokine results by intracellular protein staining and ELISA bulk protein analysis may be due to masking of subset-specific differences in overall T cell secreted protein levels or the different timepoints assessed. Increased IFNγ and IL-17 expression suggests enrichment of Th1/Th17 in BOXR1030 cells which could support a more potent anti-tumor response(32). The GOT2 byproduct aKG has been reported to preferentially expand either Th1(12) or Th17(40) T cells through epigenetic modulation of gene expression. In addition, BOXR1030 cells had a less differentiated CD27+ CD45RA+ phenotype which can improve *in vivo* persistence, while also demonstrating superior anti-GPC3 function *in vitro* in TME-like conditions (hypoxia, low glucose, and chronic stimulation). Transcriptomic analysis of BOXR1030 cells also illustrated reduced expression of pathways associated with cellular stress such as protein refolding and mTOR signaling compared to CAR control only cells. Reduced cell stress and exhaustion, enhanced production of cytokines and a less-differentiated phenotype have been shown to be associated with activity of CAR T therapies and are likely key mechanistic changes responsible for the improved antitumor activity of BOXR1030 T cells relative to CAR T cells.

In vivo, we observed improved anti-tumor activity in two xenograft models associated with enhanced BOXR1030 expansion and persistence compared to control CAR T cells. Significantly reduced levels of PD-1 and TIM-3 expression were also observed on tumor-infiltrating BOXR1030 T cells—a key readout associated with tumor volume in our models. We also did not observe any indication of toxicity or off-target expansion of BOXR1030 in normal mouse tissues, while target-specificity of BOXR1030 was observed with expansion in the GPC3+ tumor tissues.

Here, we demonstrated a mechanistic role for exogenous expression of GOT2 in the improvement of CAR T cell metabolism that was associated with changes in T cell phenotype, cytokine profile, and transcriptional profile *in vitro* leading to reduced long-term exhaustion marker expression and substantially improved antitumor efficacy of a GPC3 CAR in aggressive solid tumor xenograft models. Together, these data show that BOXR1030 is an attractive approach to targeting select solid tumors. To this end, BOXR1030 will be explored in the clinic to assess safety, dose-finding, and preliminary efficacy (NCT05120271).

Acknowledgements

The authors would like to recognize Andrew Lysaght at Immuneering for assistance with RNA-Seq analysis. The authors would like to recognize Jessica Wan for the development of the exogenous GOT2 PCR assay, and Ruchi Newman for consultation on the RNA-Seq data. The authors would like to thank all of their colleagues at Unum Therapeutics and SOTIO, LLC for feedback and critical review of data throughout the project. In particular, the authors would like to thank Jessica Sachs, Casey Judge, Amy Holbrook, and Matt Osbourne for critical review of earlier versions of the manuscript.

REFERENCES

1. June CH, Sadelain M. Chimeric Antigen Receptor Therapy. N Engl J Med. 2018;379:64–73.
2. Kershaw MH, Westwood JA, Parker LL, Wang G, Eshhar Z, Mavroukakis SA, et al. A phase I study on adoptive immunotherapy using gene-modified T cells for ovarian cancer. Clin Cancer Res. 2006;12:6106–15.
3. Morgan RA, Yang JC, Kitano M, Dudley ME, Laurencot CM, Rosenberg SA. Case report of a serious adverse event following the administration of T cells transduced with a chimeric antigen receptor recognizing ERBB2. Mol Ther. 2010;18:843–51.
4. O'Rourke DM, Nasrallah MP, Desai A, Melenhorst JJ, Mansfield K, Morrissette JJD, et al. A single dose of peripherally infused EGFRvIII-directed CAR T cells mediates antigen loss and induces adaptive resistance in patients with recurrent glioblastoma. Sci Transl Med. 2017;9.
5. Motz GT, Coukos G. Deciphering and reversing tumor immune suppression. Immunity. 2013;39:61–73.
6. Thommen DS, Schumacher TN. T Cell Dysfunction in Cancer. Cancer Cell. 2018;33:547–62.
7. Chang C-H, Qiu J, O'Sullivan D, Buck MD, Noguchi T, Curtis JD, et al. Metabolic Competition in the Tumor Microenvironment Is a Driver of Cancer Progression. Cell. 2015;162:1229–41.
8. Bengsch B, Johnson AL, Kurachi M, Odorizzi PM, Pauken KE, Attanasio J, et al. Bioenergetic Insufficiencies Due to Metabolic Alterations Regulated by the Inhibitory Receptor PD-1 Are an Early Driver of CD8(+) T Cell Exhaustion. Immunity.

2016;45:358–73.

9. Siska PJ, Beckermann KE, Mason FM, Andrejeva G, Greenplate AR, Sendor AB, et al. Mitochondrial dysregulation and glycolytic insufficiency functionally impair CD8 T cells infiltrating human renal cell carcinoma. JCI Insight. 2017;2.
10. Ma EH, Bantug G, Griss T, Condotta S, Johnson RM, Samborska B, et al. Serine Is an Essential Metabolite for Effector T Cell Expansion. Cell Metab. 2017;25:345–57.
11. Johnson MO, Wolf MM, Madden MZ, Andrejeva G, Sugiura A, Contreras DC, et al. Distinct Regulation of Th17 and Th1 Cell Differentiation by Glutaminase-Dependent Metabolism. Cell. 2018;175:1780-1795.e19.
12. Klysz D, Tai X, Robert PA, Craveiro M, Cretenet G, Oburoglu L, et al. Glutamine-dependent α-ketoglutarate production regulates the balance between T helper 1 cell and regulatory T cell generation. Sci Signal. 2015;8:ra97.
13. Geiger R, Rieckmann JC, Wolf T, Basso C, Feng Y, Fuhrer T, et al. L-Arginine Modulates T Cell Metabolism and Enhances Survival and Anti-tumor Activity. Cell. 2016;167:829-842.e13.
14. Son J, Lyssiotis CA, Ying H, Wang X, Hua S, Ligorio M, et al. Glutamine supports pancreatic cancer growth through a KRAS-regulated metabolic pathway. Nature. 2013;496:101–5.
15. van Karnebeek CDM, Ramos RJ, Wen X-Y, Tarailo-Graovac M, Gleeson JG, Skrypnyk C, et al. Bi-allelic GOT2 Mutations Cause a Treatable Malate-Aspartate Shuttle-Related Encephalopathy. Am J Hum Genet. 2019;105:534–48.
16. Bailis W, Shyer JA, Zhao J, Canaveras JCG, Al Khazal FJ, Qu R, et al. Distinct modes of mitochondrial metabolism uncouple T cell differentiation and function. Nature.

2019;571:403–7.

17. Chisolm DA, Savic D, Moore AJ, Ballesteros-Tato A, León B, Crossman DK, et al. CCCTC-Binding Factor Translates Interleukin 2- and α-Ketoglutarate-Sensitive Metabolic Changes in T Cells into Context-Dependent Gene Programs. Immunity. 2017;47:251-267.e7.

18. Hiemer S, Jatav S, Jussif J, Alley J, Lathwal S, Piotrowski M, et al. Integrated Metabolomic and Transcriptomic Profiling Reveals Novel Activation-Induced Metabolic Networks in Human T Cells. SSRN Electron J. 2019

19. Bettonville M, d'Aria S, Weatherly K, Porporato PE, Zhang J, Bousbata S, et al. Long-term antigen exposure irreversibly modifies metabolic requirements for T cell function. Elife. 2018;7.

20. Ho M, Kim H. Glypican-3: a new target for cancer immunotherapy. Eur J Cancer. 2011;47:333–8.

21. Baumhoer D, Tornillo L, Stadlmann S, Roncalli M, Diamantis EK, Terracciano LM. Glypican 3 expression in human nonneoplastic, preneoplastic, and neoplastic tissues: a tissue microarray analysis of 4,387 tissue samples. Am J Clin Pathol. 2008;129:899–906.

22. Ishiguro T, Sano Y, Komtsu SI, Kamata-Sakura M, Kaneko A, Kinoshita Y, et al. An anti-glypican 3/CD3 bispecific T cell-redirecting antibody for treatment of solid tumors. Sci Transl Med. 2017;9.

23. Moek KL, Fehrmann RSN, van der Vegt B, de Vries EGE, de Groot DJA. Glypican 3 Overexpression across a Broad Spectrum of Tumor Types Discovered with Functional Genomic mRNA Profiling of a Large Cancer Database. Am J Pathol. 2018;188:1973–81.

24. Lu C, Rong D, Zhang B, Zheng W, Wang X, Chen Z, et al. Current perspectives on the

immunosuppressive tumor microenvironment in hepatocellular carcinoma: challenges and opportunities. Mol Cancer. 2019;18:130.

25. Wang X, He Q, Shen H, Xia A, Tian W, Yu W, et al. TOX promotes the exhaustion of antitumor CD8+ T cells by preventing PD1 degradation in hepatocellular carcinoma. J Hepatol. 2019;71:731–41.

26. Engels B, Cam H, Schüler T, Indraccolo S, Gladow M, Baum C, et al. Retroviral vectors for high-level transgene expression in T lymphocytes. Hum Gene Ther. 2003;14:1155–68.

27. Cerami E, Gao J, Dogrusoz U, Gross BE, Sumer SO, Aksoy BA, et al. The cBio cancer genomics portal: an open platform for exploring multidimensional cancer genomics data. Cancer Discov. 2012;2:401–4.

28. Gao J , Aksoy BA, Dogrusoz U, Dresdner G, Gross B, Sumer SO, et al. Integrative analysis of complex cancer genomics and clinical profiles using the cBioPortal. Sci Signal. 2013;6.

29. Khan O, Giles JR, McDonald S, Manne S, Ngiow SF, Patel KP, et al. TOX transcriptionally and epigenetically programs CD8+ T cell exhaustion. Nature [Internet]. Nature Publishing Group; 2019 [cited 2021 Jul 31];571:211–8. Available from: http://www.nature.com/articles/s41586-019-1325-x

30. Seo H, Chen J, González-Avalos E, Samaniego-Castruita D, Das A, Wang YH, et al. TOX and TOX2 transcription factors cooperate with NR4A transcription factors to impose CD8+ T cell exhaustion. Proc Natl Acad Sci U S A. 2019;116:12410–5.

31. Gerlach C, Moseman EA, Loughhead SM, Garg R, De La Torre JC, Von UH, et al. The Chemokine Receptor CX3CR1 Defines Three Antigen-Experienced CD8 T Cell Subsets with Distinct Roles in Immune Surveillance and Homeostasis Article The Chemokine

Receptor CX3CR1 Defines Three Antigen-Experienced CD8 T Cell Subsets with Distinct Roles in Immune Surveillance and Homeostasis. Immunity. 2016;45:1270–84.

32. Majchrzak K, Nelson MH, Bailey SR, Bowers JS, Yu X-Z, Rubinstein MP, et al. Exploiting IL-17-producing CD4+ and CD8+ T cells to improve cancer immunotherapy in the clinic. Cancer Immunol Immunother. 2016;65:247.

33. Araki K, Turner AP, Shaffer VO, Gangappa S, Keller SA, Bachmann MF, et al. mTOR regulates memory CD8 T-cell differentiation. Nature. 2009;460:108–12.

34. Alizadeh D, Wong RA, Yang X, Wang D, Pecoraro JR, Kuo C-F, et al. IL15 Enhances CAR-T Cell Antitumor Activity by Reducing mTORC1 Activity and Preserving Their Stem Cell Memory Phenotype. Cancer Immunol Res. 2019;7:759–72.

35. Zhao Z, Condomines M, van der Stegen SJC, Perna F, Kloss CC, Gunset G, et al. Structural Design of Engineered Costimulation Determines Tumor Rejection Kinetics and Persistence of CAR T Cells. Cancer Cell. 2015;28:415–28.

36. Scharping NE, Menk A V, Moreci RS, Whetstone RD, Dadey RE, Watkins SC, et al. The Tumor Microenvironment Represses T Cell Mitochondrial Biogenesis to Drive Intratumoral T Cell Metabolic Insufficiency and Dysfunction. Immunity. 2016;45:374–88.

37. Patsoukis N, Bardhan K, Chatterjee P, Sari D, Liu B, Bell LN, et al. PD-1 alters T-cell metabolic reprogramming by inhibiting glycolysis and promoting lipolysis and fatty acid oxidation. Nat Commu. 2015;6:6692.

38. Macintyre AN, Gerriets VA, Nichols AG, Michalek RD, Rudolph MC, Deoliveira D, et al. The glucose transporter Glut1 is selectively essential for CD4 T cell activation and effector function. Cell Metab. 2014;20:61–72.

39. Ron-Harel N, Ghergurovich JM, Notarangelo G, LaFleur MW, Tsubosaka Y, Sharpe AH,

et al. T Cell Activation Depends on Extracellular Alanine. Cell Rep. 2019;28:3011-3021.e4.

40. Xu T, Stewart KM, Wang X, Liu K, Xie M, Ryu JK, et al. Metabolic control of TH17 and induced Treg cell balance by an epigenetic mechanism. Nature. 2017;548:228–33.

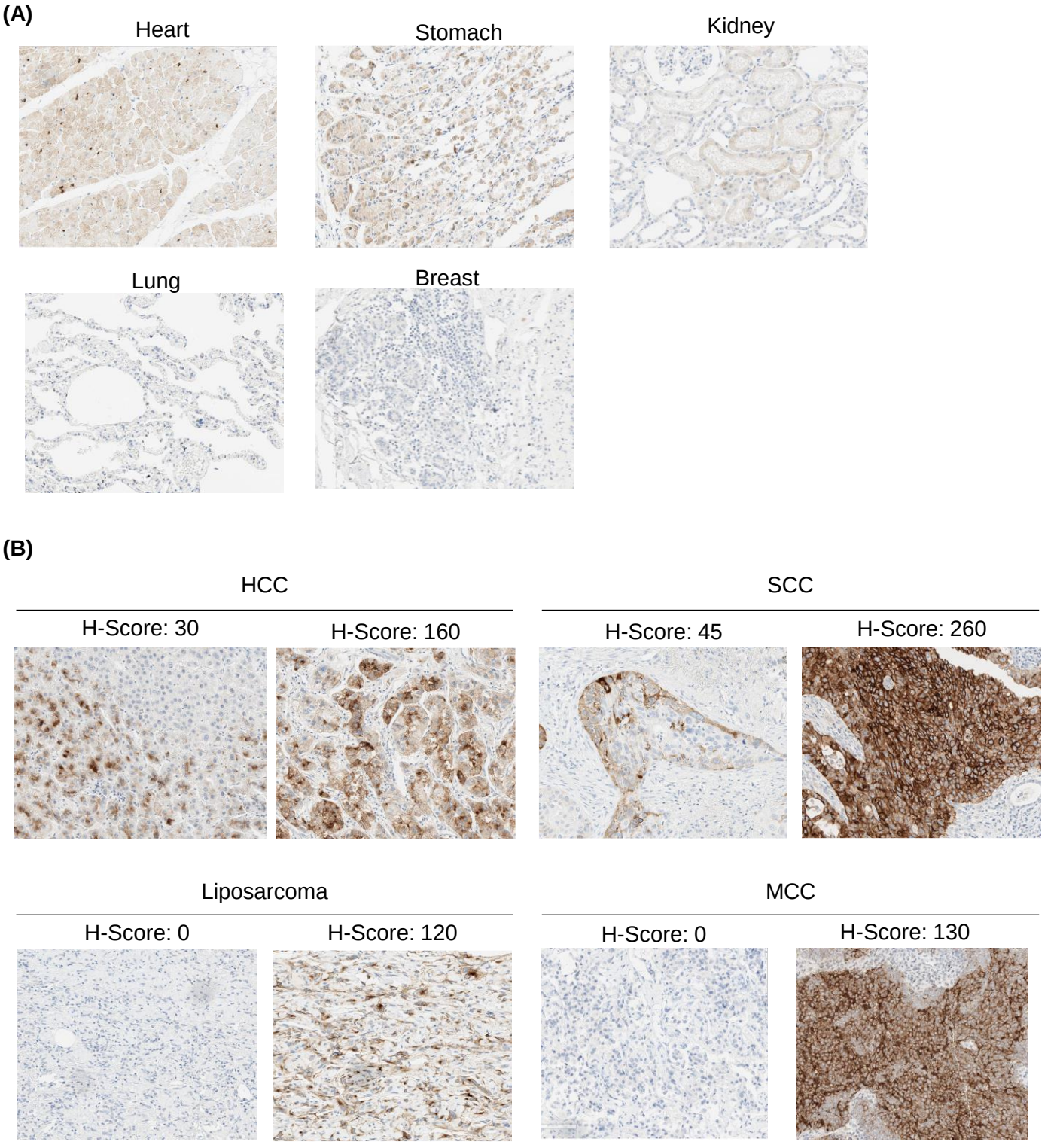

Figure 1. GPC3 target expression in human normal and tumor tissues by IHC. (A) Immunohistochemical staining of normal healthy TMA for GPC3 expression. Representative images (20x magnification) of different organs with different levels of GPC3 are shown (B) IHC staining of tissues from hepatocellular carcinoma (HCC), squamous cell lung cancer (SCC), Merkel cell carcinoma (MCC) and liposarcoma patients for GPC3 expression. Representative images (20x magnification) show samples with different levels of GPC3 (and H-scores).

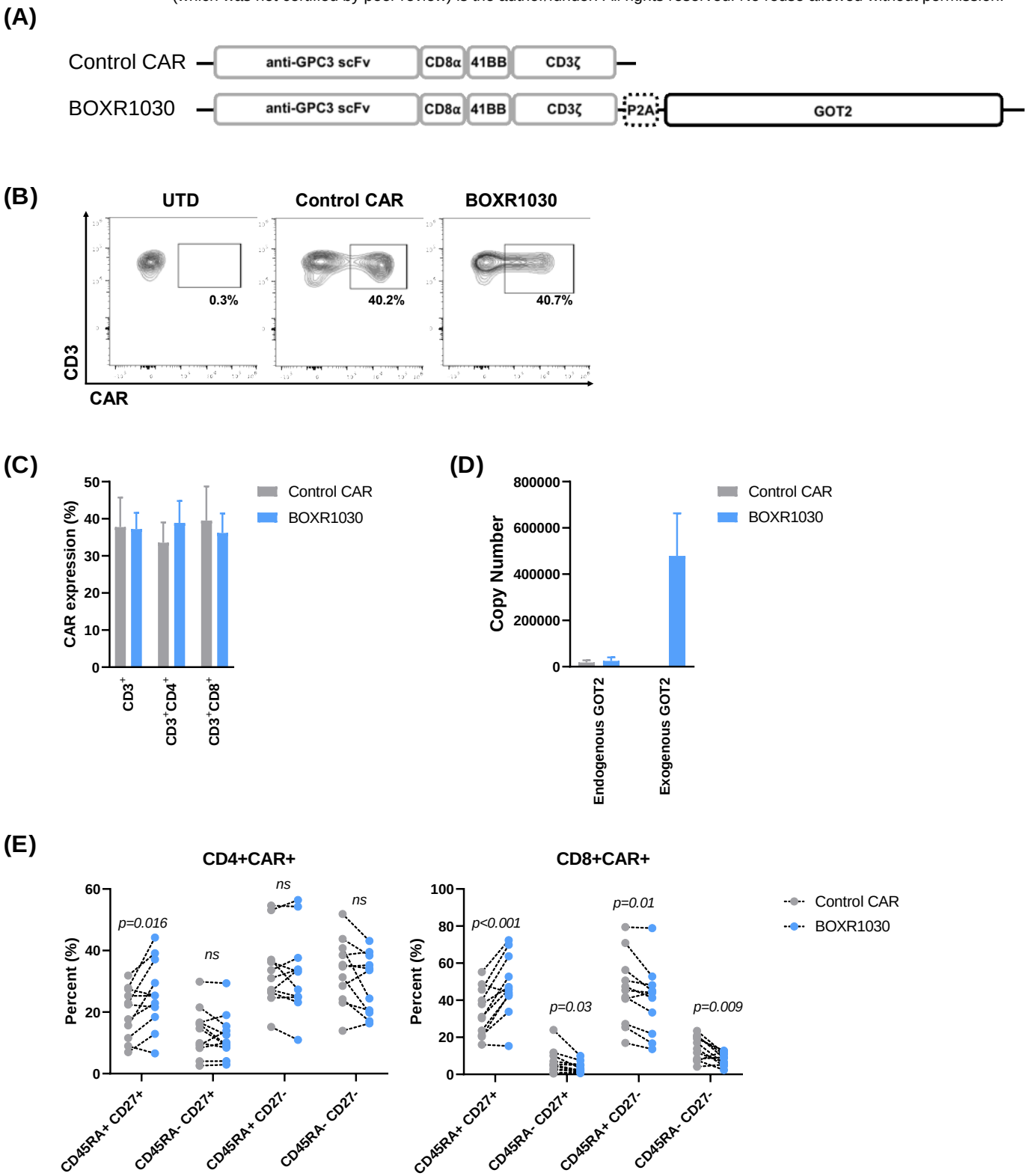

Figure 2. Co-expression of GPC3-targeted CAR with exogenous GOT2 in BOXR1030 T cells (A) Depiction of expression construct and domains for the GPC3 CAR and BOXR1030 used in studies. (B) Representative surface expression of the anti-GPC3 scFv following transduction, measured on day 9 by flow cytometry from a single donor. (C) Summarized CAR expression by flow cytometry for n=5 healthy donors. (D) mRNA copy number of endogenous and exogenous (codon optimized) GOT2 measured by qPCR (n= 3 donors). (E) The frequency of CD45RA+ CD27+, CD45RA+ CD27-, CD45RA- CD27+, and CD45RA- CD27- T cells in the indicated subsets at baseline (n=11 healthy donors; no stimulation). P-values were determined by paired t-test. Data represented as mean+/- standard deviation (SD).

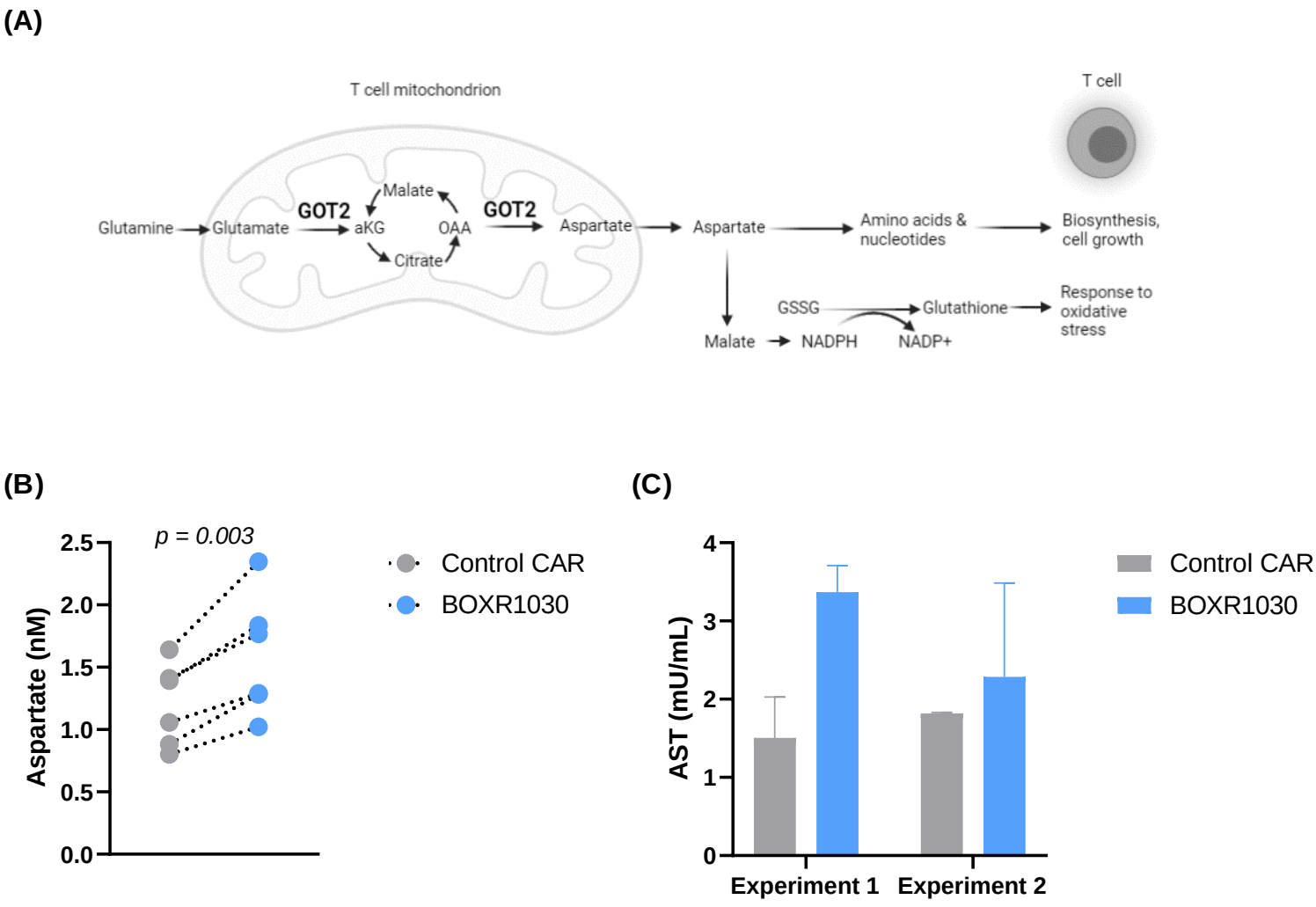

Figure 3. AST enzymatic activity in BOXR1030 CAR T cells. (A) Schematic describing the role of GOT2 in mitochondrial conversion of glutamate to aKG and OAA to aspartate. Image created with biorender.com. (B) Intracellular aspartate levels were measured using a plate-based colorimetric assay comparing BOXR1030 and control CAR T cells under non-stimulated conditions. (C) BOXR1030 and control CAR T cells were activated for 8 hours with GPC3+ Hep3B target cells and evaluated for AST activity. Data represented as mean +/- SD of two technical replicates

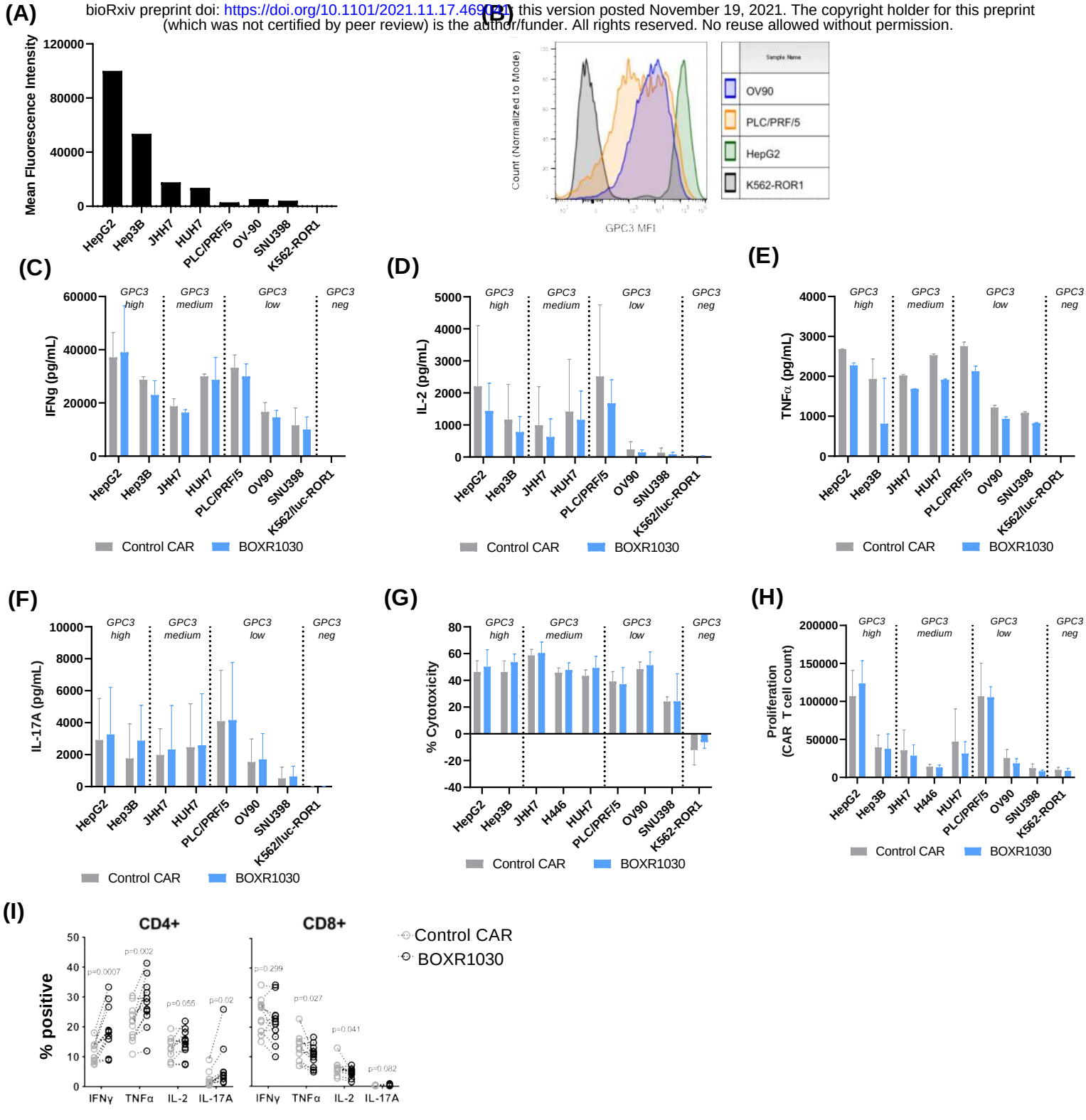

Figure 4. *In vitro* BOXR1030 activity. (A) Expression of GPC3 target antigen on target cell lines were measured by flow cytometry and represented as median fluorescence intensity (MFI). (B) Histogram plots of GPC3 MFI for selected cell lines. (C-F) T cell cytokine release of BOXR1030 and control CAR T cells was measured by ELISA following co-culture with target cell lines for 24 hours. Results for IFN-g (C) and IL-2 (D) are the averages across 3 donors, and error bars indicate SD. Results for TNF-a (E) and IL-17A (F) are for a single donor, and error bars indicate SD between technical replicates. (G) Target cell cytotoxicity was measured with a luciferase-based assay, and percent cytotoxicity was normalized to samples treated with untransduced T cells following 24 hours of co-culture (n=3 donors, error bars indicate SD). (H) T cell proliferation was evaluated after a 7 day incubation with target cell lines. CAR+ T cell counts were measured by flow cytometry. (n= 3 donors, error bars indicate SD). (I) Intracellular cytokine levels were measured by flow cytometry in CD4+ and CD8+ T cells (n=10, error bars indicate SEM)

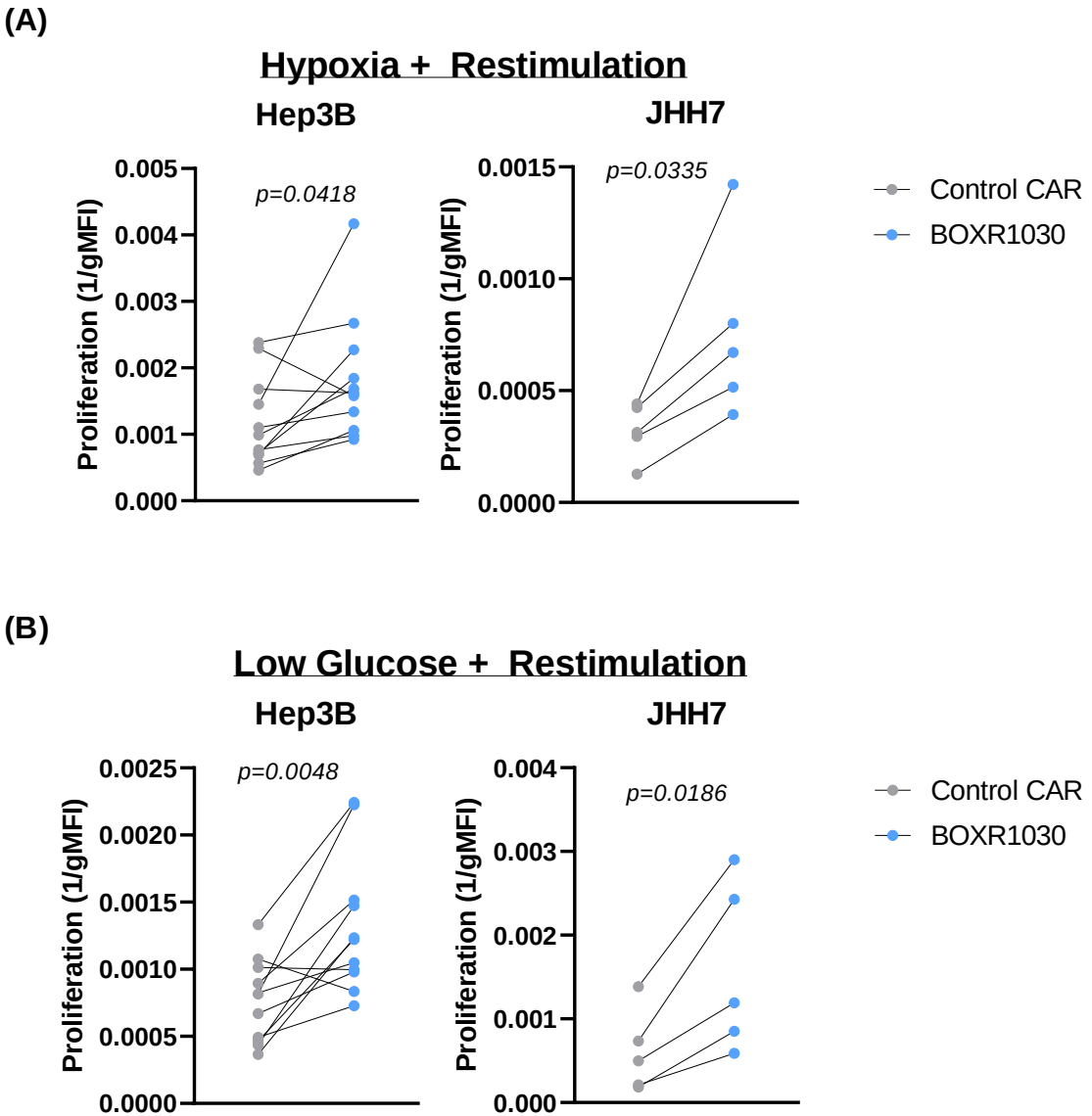

Figure 5. *In vitro* activity of BOXR1030 under conditions simulating the solid tumor microenvironment. BOXR1030 or control CAR T cells were repeat stimulated with GPC3+ target cell lines on day 0 and on day 7 in hypoxic conditions (A) or low glucose conditions (B). (A and B) The gMFI of CellTrace Violet (CTV) was measured for BOXR1030 and control CAR stimulated with target cells in the indicated culture conditions and proliferation was plotted as 1/gMFI. (n=5 for JHH7 stimulated conditions and n=11 for Hep3B stimulated conditions, statistical analysis was performed using a 2-tailed paired t-test, and p-values <0.05 were considered statistically significant).

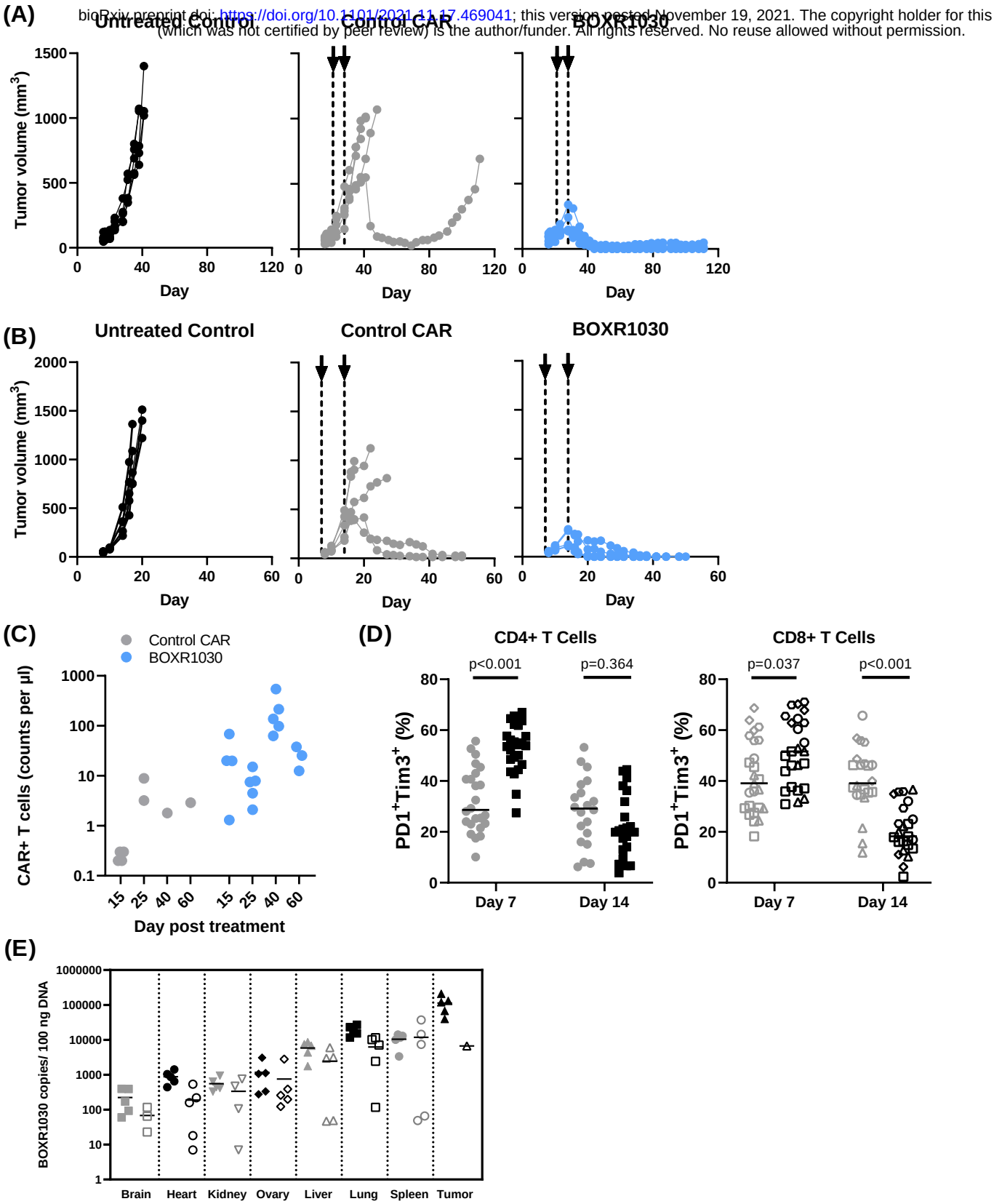

Figure 6. *In vivo* anti-tumor activity of BOXR1030 T cells. (A) Hep3B tumor-bearing NSG mice were treated with two doses of 2 x 10^6 CAR+ control or BOXR1030 T cells (dosing days indicated by arrows) and tumor volumes were measured over the course of 110 days. (B) JHH7 tumor-bearing mice were treated with two doses of 5 x 10^6 CAR+ control or BOXR1030 T cells (dosing days indicated by arrows) and tumor volumes were measured out to 50 days. (C) CAR+ T cells were measured in peripheral blood of Hep3G tumor bearing mice on days 15, 25, 40 and 60 post T cell treatment and data are reported as counts per ul of blood. (D) Percent PD1+TIM3+CD4+ and PD1+TIM3+CD8+ tumor infiltrating T cells were measured by FACS on days 7 and 14 following T cell administration. (E) Biodistribution of BOXR1030 T cells was measured in mouse tissues by qPCR at days 15 and 45 post treatment. Data are reported as BOXR1030 copies / 100ng DNA.

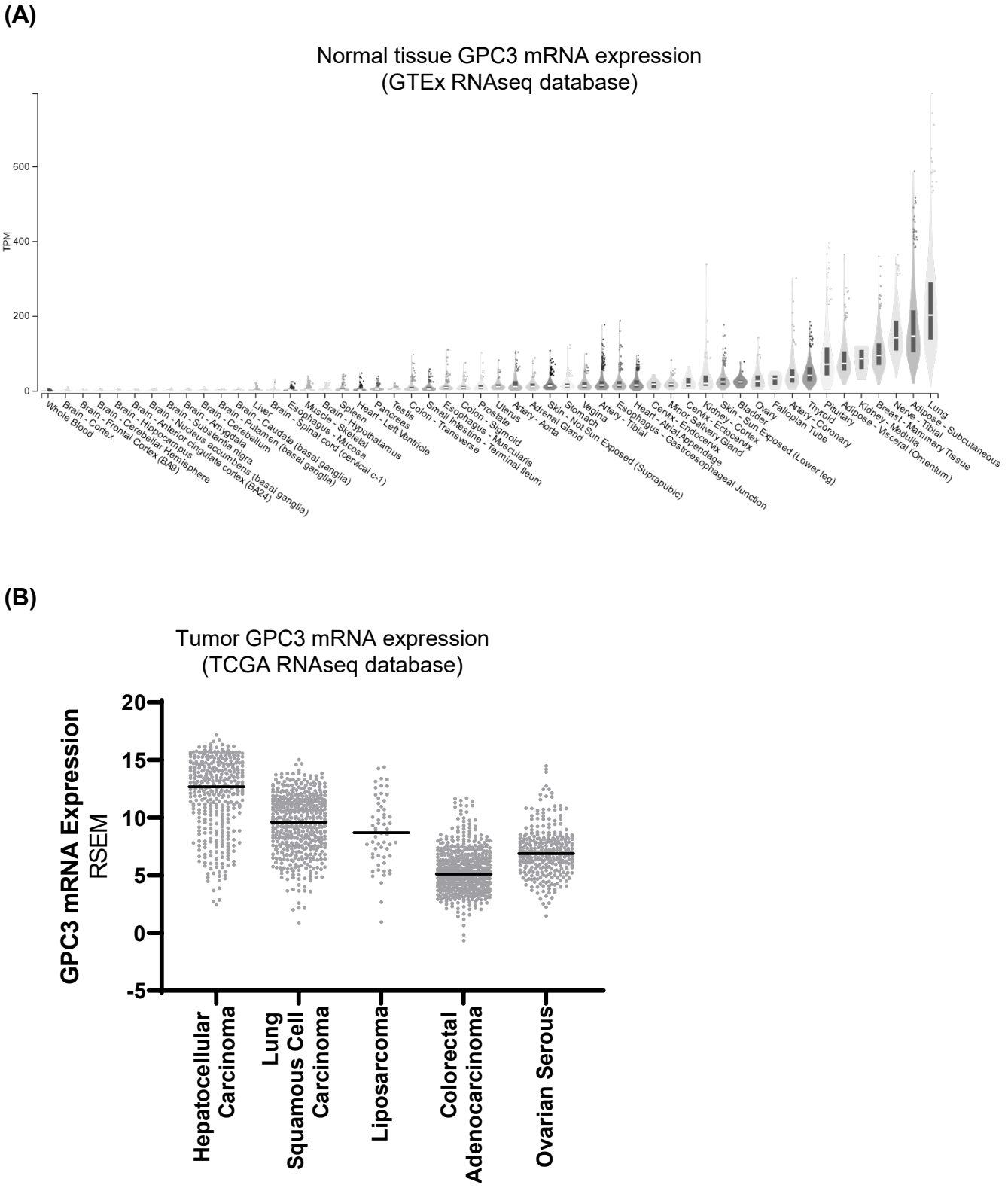

Supplementary Figure 1. GPC3 mRNA expression in human normal and tumor tissues. (A) GPC3 mRNA expression in normal tissues was analyzed from the GTEx RNAseq database. Data are shown as transcripts per million (TPM) and tissues are rank-ordered by median expression. (B) GPC3 mRNA expression in selected tumor indications was analyzed from the TCGA RNAseq database and data are shown as RSEM.

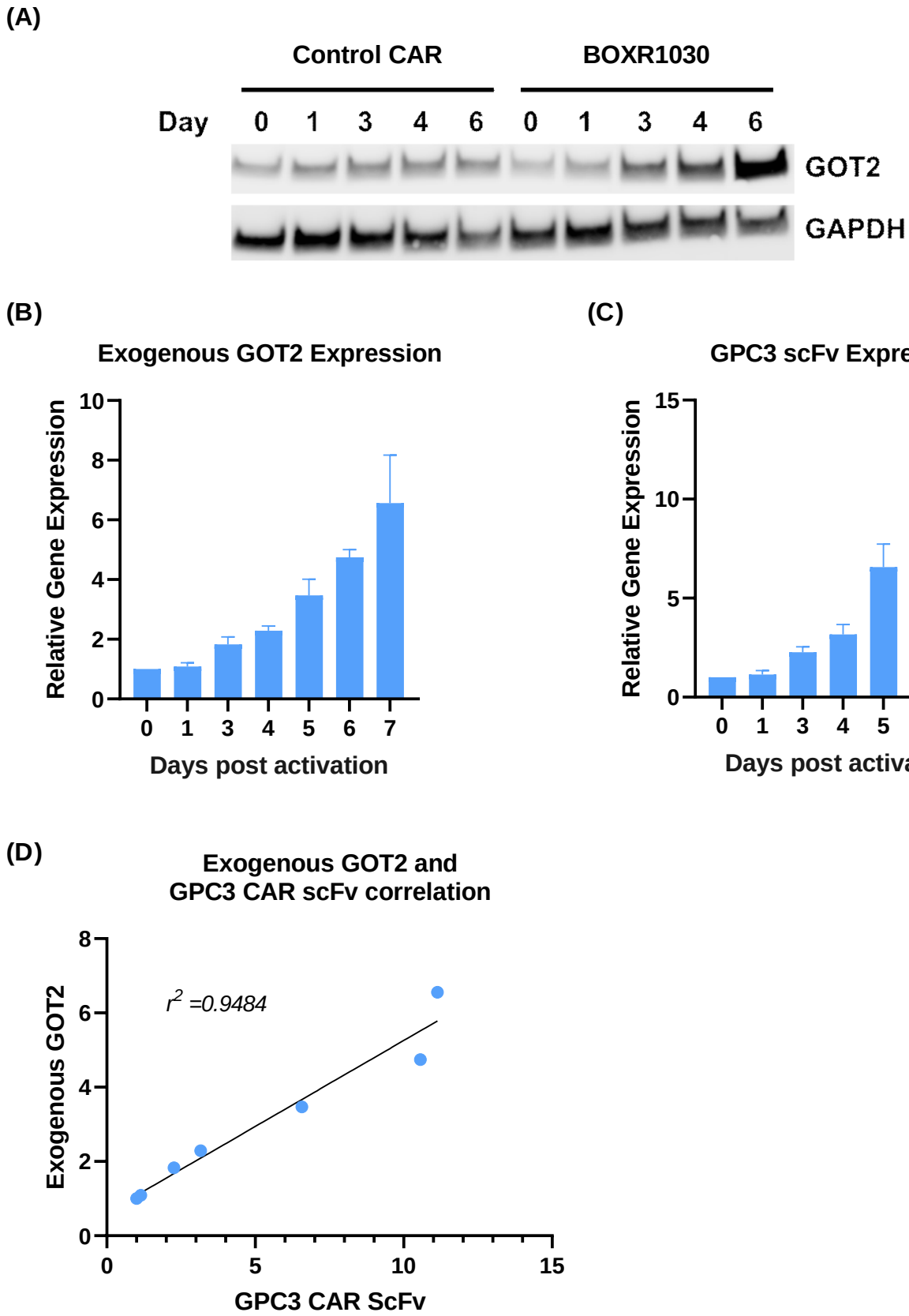

Supplementary Figure 2. CAR and GOT2 expression following antigen stimulation Control and BOXR1030 T cells were stimulated with plate bound GPC3 antigen over the course of 7 days. (A) GOT2 protein expression was measured by western blot and GAPDH serves as a loading control. (B) Exogenous GOT2 mRNA and (C) GPC3 CAR scFv mRNA were measured by qPCR. (D) Correlation plot comparing GPC3 scFv mRNA expression and GOT2 transgene mRNA expression (all data are from a single representative donor).

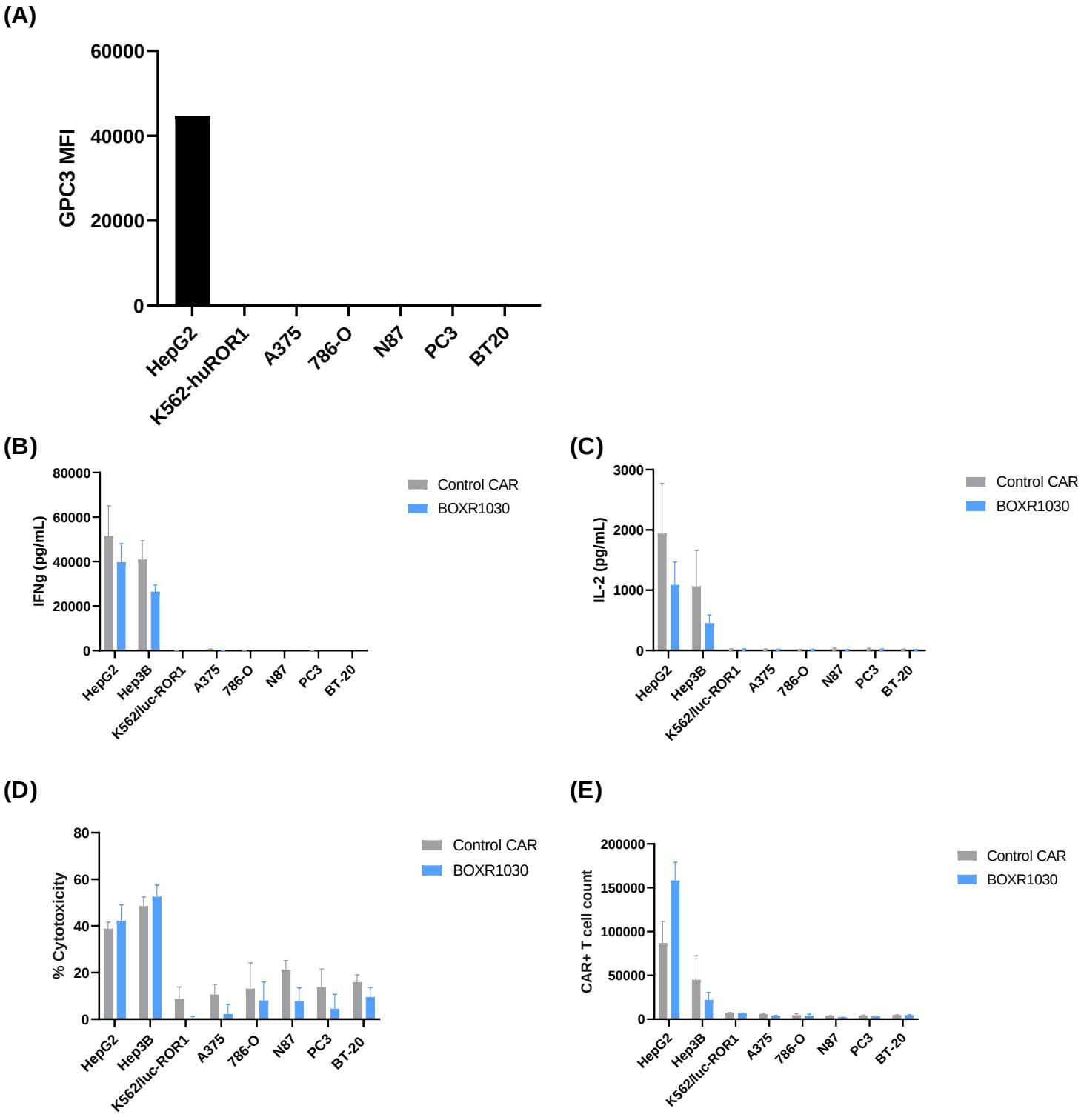

Supplementary Figure 3. Specificity of GPC3 CAR (A) GPC3 target expression was measured by flow cytometry for several antigen negative cell lines. (B-E) Control CAR or BOXR1030 T cells were cocultured with a panel of antigen negative cell lines and (B) IFNg and (C) IL-2 cytokine secretion were measured by ELISA and cytotoxicity (D) and proliferation (E) were measured to confirm specificity for the target. HEPG2 cells served as a positive control.

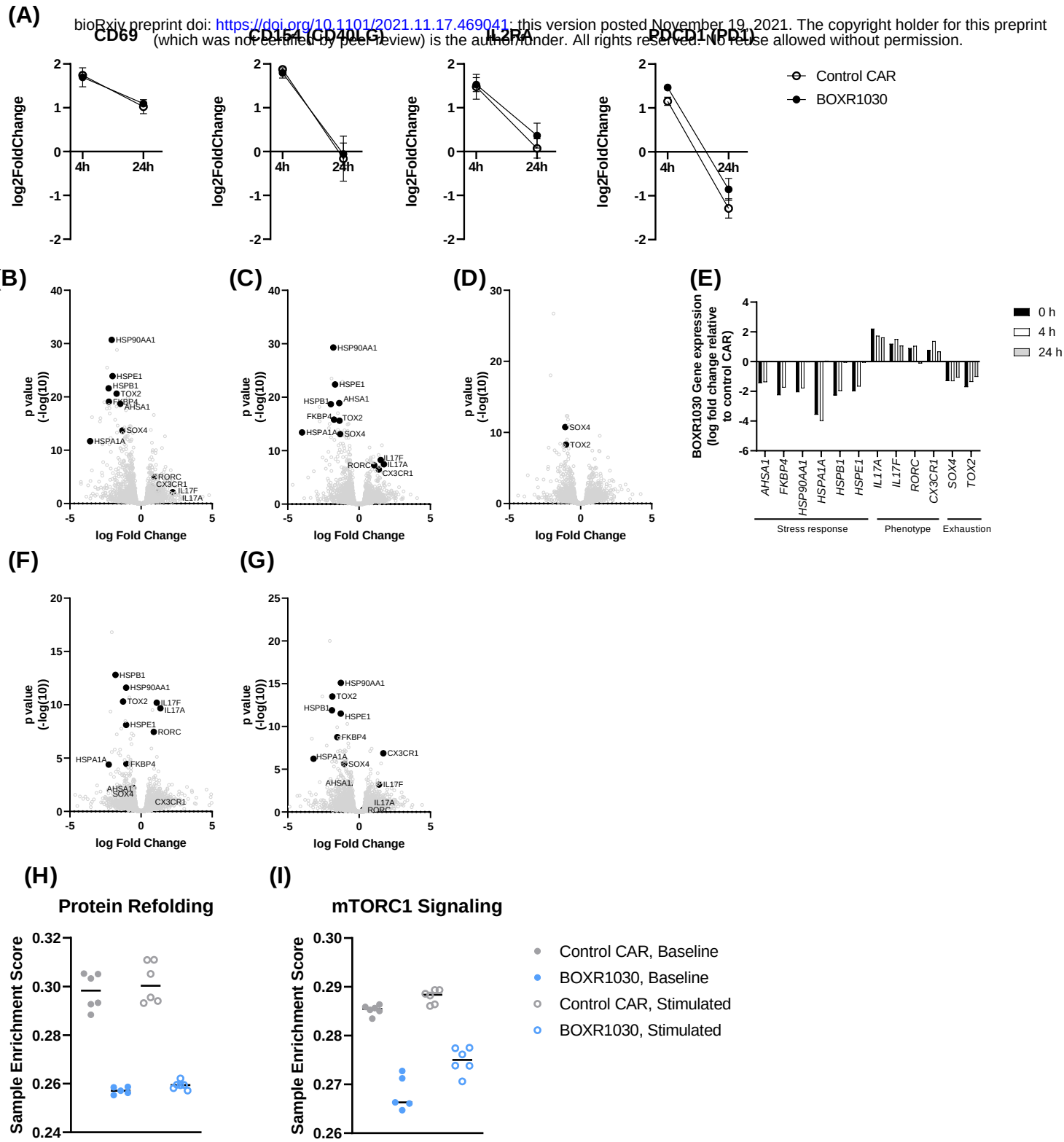

Supplementary Figure 4. RNAseq analysis of BOXR1030 T cells. BOXR1030 or control CAR T cells were stimulated for 0, 4 or 24hrs with plate-bound GPC3 antigen and assessed for global changes in RNA expression by RNAseq. (A) RNA expression of activation makers *CD69*, *CD154(CD40LG)*, *IL2RA(CD25)* and *PDCD1(PD1)* following stimulation for 4 and 24 hours. Data are represented as log2 fold change from baseline (time 0, unstimulated). (B-D) Differential gene expression at (B) baseline (C) 4 hours and (D) 24 hours represented as volcano plots comparing log fold change BOXR1030 relative to control CAR T cells. (E) Selected genes from B-D plotted in bar graph format. (F,G) Differential gene expression in CD4 (F) and CD8 (G) T cell populations following 4 hours of antigen stimulation. Data are plotted as log fold change BOXR1030 T cells relative to control T cells for each subset. (H, I) Gene set enrichment score for (H) protein refolding and (I) mTORC1 signaling for control CAR and BOXR1030 unstimulated and stimulated (4 h) cells. (n=2 donors, 3 technical repeats for each condition and each donor).

Supplementary Table 1. Summary of TMA IHC Staining.

TMA indication	Number of cases	Number of cases with H score ≥ 30
HCC	70	51
Lung cancer	75 (10 small cell undifferentiated carcinoma, 33 squamous cell carcinoma, 32 adenocarcinoma)	Only scored squamous cell carcinoma 9
Liposarcoma	80 (30 pleiomorphic liposarcoma, 25 cases of myxoid/round liposarcoma, 15 well-differentiated liposarcoma 10 other liposarcomas)	11 all liposarcoma 8 (myxoid/round liposarcoma only)
Ovarian cancer	77 (15 cases of cystadenoma 31 serous carcinoma, 6 mucinous adenocarcinoma, 10 endometrioid adenocarcinoma 15 others on ovarian cancer progression spectrum)	Only scored serous ovarian cancer 2 (serous ovarian cancer)
Colon adenocarcinoma	80	0

Supplementary Table 2. Summary of Tissue Section IHC Staining.

Indication	Number of cases	Number of cases with H score ≥ 30
HCC	40	25
SCC	40	15
Liposarcoma (MRCLS)	40 (20)	12 (7)
MCC	20	14